AIP Applied Physics Letters

Crucial role played by interface and oxygen content in magnetic properties of ultrathin manganite films

Cong Wang, Kui-juan Jin, Lin Gu, Hui-bin Lu, Shan-ming Li et al.

Citation: Appl. Phys. Lett. **102**, 252401 (2013); doi: 10.1063/1.4812302
View online: http://dx.doi.org/10.1063/1.4812302
View Table of Contents: http://apl.aip.org/resource/1/APPLAB/v102/i25
Published by the AIP Publishing LLC.

Crucial role played by interface and oxygen content in magnetic properties of ultrathin manganite films

Cong Wang, Kui-juan Jin,[a] Lin Gu, Hui-bin Lu, Shan-ming Li, Wen-jia Zhou, Rui-qiang Zhao, Hai-zhong Guo, Meng He, and Guo-zhen Yang
Beijing National Laboratory for Condensed Matter Physics, Institute of Physics, Chinese Academy of Sciences, Beijing 100190, China

(Received 1 April 2013; accepted 12 June 2013; published online 24 June 2013)

Unusual magnetic properties are found in ultrathin $La_{0.9}Sr_{0.1}MnO_3$ films by systematically investigating the films with the thicknesses varying from 200 to 6 unit cells. Post annealing in oxygen can significantly enhance the Curie temperature and saturation magnetization by complementing oxygen vacancies. We observe that oxygen vacancies around the surfaces are much more than those close to the interfaces using an aberration-corrected scanning transmission electron microscopy for both the as-grown and post-annealed ultrathin films. The Curie temperature up to 325 K, much higher than that of the bulk, is found in the annealed films with the thickness of 50 unit cells. © *2013 AIP Publishing LLC*. [http://dx.doi.org/10.1063/1.4812302]

Some intriguing states and exotic phenomena appear at the interfaces where perovskite oxides with different structural and electronic properties meet,[1–3] such as the formation of a high-mobility two-dimensional electron gas at the interface of two insulators[4] and the emergence of ferromagnetism at the interface of two non-ferromagnetic materials.[5] Perovskite-type manganite has attracted much attention as a promising candidate for ferromagnetic electrodes in the magnetic tunneling junction (MTJ), as it features highly polarized conducting electrons around the Femi surface and high Curie temperature.[6,7] Since the tunneling magnetoresistance (TMR) are dominated by the electrons tunneling through a thin insulating layer between two manganite layers, the ultrathin interface region of manganite layers with a thickness of several unit cells (u.c.) was found to be crucial to the performance of the MTJs.[8] A lot of works have shown that the interface region of manganite exhibits essential deviations from the bulk in both crystal and electronic structures,[9–12] such as strain-induced structure distortion[13] and spin canting.[14] In particular, the presence of a so-called "dead layer" when the thickness of manganite films drops down to a certain value leads to the decrease of spin polarization and the depression of magnetic and transport properties.[15] More recently, the ultimate photo-voltage in manganite-based heterostructures with a critical film thickness was discovered,[16] which indicates that more intriguing properties may yet not be exposed, especially in the ultrathin films of perovskite oxides. In this paper, we present a systematic investigation on the structural and magnetic properties of the $La_{0.9}Sr_{0.1}MnO_3$ (LSMO) films with the thicknesses varying from several hundred to 6 u.c. to provide more insight into the physics of the interface region of manganite. Oxygen vacancies around the surfaces are found much more than those close to the interfaces in the ultrathin films, which can be greatly complemented by post anneal in oxygen with a significant enhancement of the Curie temperature and saturation magnetization. The highest Curie temperature (up to 325 K), much higher than the bulk value (~140 K), is found in the annealed films with the thickness of 50 u.c. These results will promote the understanding on the crucial influence of oxygen vacancies and interfaces on the fundamental physics and the functionality of manganite ultrathin films.

$La_{0.9}Sr_{0.1}MnO_3$ films were deposited on single-crystalline substrates of $SrTiO_3$ (001) (STO) at 650 °C with the oxygen pressure of 5×10^{-2} Pa by a laser molecular beam epitaxy system using a XeCl excimer laser (wavelength of 308 nm, pulse width of 20 ns, energy density of 2 J cm^{-2}, repetition of 2 Hz). The epitaxy and thicknesses of the LSMO films were monitored by *in situ* reflective high-energy electron diffraction. The crystal structure was identified by high-resolution Synchrotron X-ray diffractometry by the BL14B1 beam line of Shanghai Synchrotron Radiation Facility (SSRF), using a 1.24 Å X-rays with a Huber 5021 six-axis diffractometry. The results from the synchrotron-based X-ray diffraction (SXRD) indicate that the *c*-axis lattice constant of our LSMO films decreases from 4.00 to 3.93 Å with the film thickness decreasing from 200 to 10 u.c.

Annular-bright-field (ABF) imaging was executed using an ARM-200F (JEOL, Tokyo, Japan) scanning transmission electron microscope (STEM) operated at 200 kV with a CEOS Cs corrector (CEOS GmbH, Heidelberg, Germany) to cope with the probe-forming objective spherical aberration. The attainable resolution of the ABF imaging is better than 80 pm to resolve individual oxygen atomic column with an illumination semiangle of 25 mrad and the corresponding collection angle of 12–25 mrad. Since the contrast of ABF micrograph is proportional to $Z^{1/3}$ and is extremely sensitive to light atoms, oxygen vacancies can be detected at atomic scale, which is of great difficulty to achieve via other methods. The magnetic field was applied along the film surfaces during the measurements of magnetic properties in the physical property measurement system (Quantum design) with a vibrating sample magnetometer.

[a]Author to whom correspondence should be addressed. Electronic mail: kjjin@iphy.ac.cn.

The hysteresis loops (10 K) and temperature-dependent magnetization (200 Oe, field cooling) of the as-grown films were shown in Figures 1(a) and 1(b), respectively. The Curie temperature (T_C) and saturation magnetization (M_S) at 10 K of these films deduced from Figures 1(a) and 1(b) were plotted in Figure 1(c). Here, T_C is defined as the temperature where (dM/dT) reaches the extremum, and M_S is defined as the magnetization under the magnetic field H of 10 kOe. The relatively small T_C and unusually large c-axis lattice constant, compared to the typical values of about 140 K and 3.87 Å for the $La_{0.9}Sr_{0.1}MnO_3$ bulk, respectively,[12,17] can be related to the existence of the interface effect and oxygen vacancies in these films, which is quite common for the oxygen pressure we employed during deposition.[18] The decrease of the c-axis lattice constant with the decreasing thickness of LSMO films should be ascribed to the less oxygen vacancies in the thinner LSMO films due to the extraction of oxygen from STO substrates around the interface, which is supported by the aberration-corrected STEM results showing few oxygen vacancies existing at the interface region of the LSMO films. The strain caused by the lattice mismatch of LSMO and STO should also play a certain role in this phenomenon. Both T_C and M_S decrease monotonously while the film thickness varies from 200 to 8 u.c., and the magnetic moment of the ultrathin films with the thickness of 6 u.c. cannot be distinguished from the environment in the physical property measurement system. This decay in T_C and M_S can be attributed to the strain effects at the interface[19] and structure distortion,[13] since it was proposed that the decay in T_C and M_S was induced by the stretched Mn-O bonds[20] and the spin canting[14] around the LSMO/STO interfaces, respectively, due to the tensile strain from STO substrates.

It has been reported that oxygen vacancies can shift the valence band and lower the spin polarization and conductivity of manganites,[21–23] which would usually jeopardize their applications in functional devices. Recent progress in aberration-corrected electron optics has significantly enhanced the performance of electron microscopes, enabling identification of individual light atoms such as oxygen.[24,25] To investigate the crucial role played by oxygen vacancies in the LSMO films, we exploited an aberration-corrected ABF imaging technique. Figures 2(a)–2(c) display the cross-sectional ABF micrographs of the LSMO film with the thickness of 16 u.c. taken by an aberration-corrected STEM, while Figures 2(d)–2(f) show the corresponding line profiles along the Mn-O-Mn chains (the dark cyan bars) in Figures 2(a)–2(c), respectively. From the line profiles of the ABF micrographs in Figure 2, oxygen vacancies at the Mn-O-Mn chains were found to undertake a drastic concentration distribution along the growth direction, in which oxygen vacancies existing around the surfaces are much more than those close to the interfaces. The sufficiency of oxygen at the interface region of LSMO film should come from the fact that some oxygen ions were extracted from the STO substrate. Since there exist few oxygen vacancies at the interface region of LSMO, it can be well understood that the decrease of the c-axis lattice constant with the decreasing thickness of the LSMO films should be attributed to the less oxygen vacancies in the thinner LSMO films, which is confirmed by the comparison among the ABF images of the LSMO films with different thicknesses. Since the existence of oxygen vacancies was found to distort the lattice and suppressed the magnetization of manganite films, we argue that the dead layer would be thicker with more oxygen vacancies, which indicates that

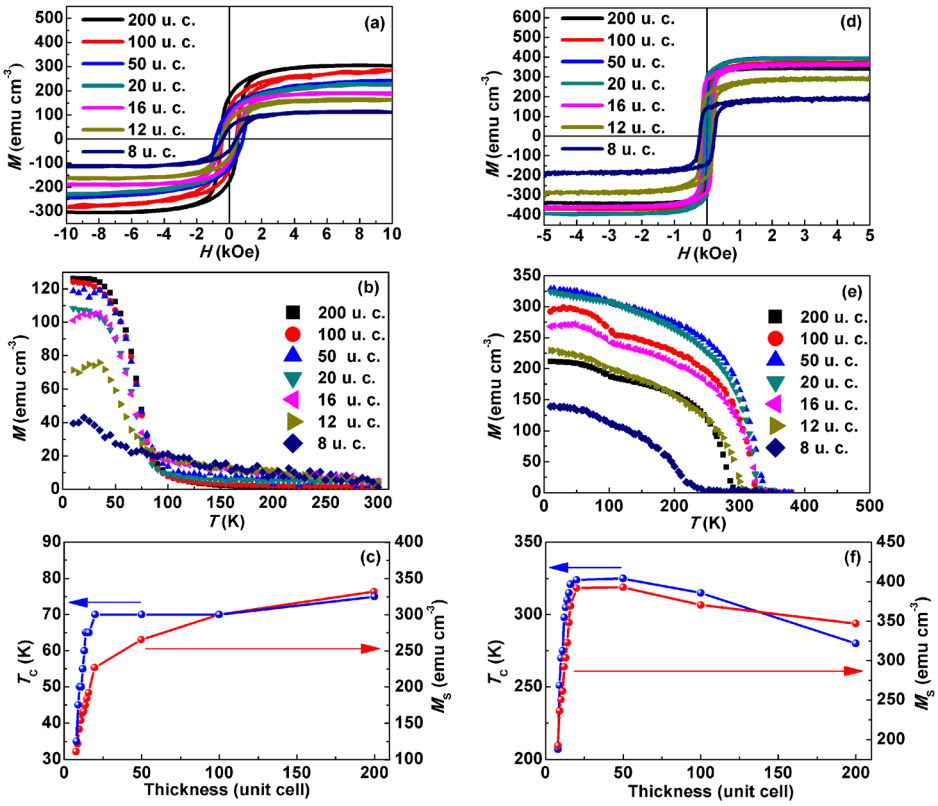

FIG. 1. The hysteresis loops (10 K) (a) and temperature-dependent magnetization (200 Oe, field cooling) (b) of the as-grown LSMO films. The thickness-dependent saturation magnetization (10 K) (red) and Curie temperature (blue) of the as-grown LSMO films (c) and the annealed LSMO films (f). The hysteresis loops (10 K) (d) and temperature-dependent magnetization (20 Oe, field cooling) (e) of the annealed LSMO films.

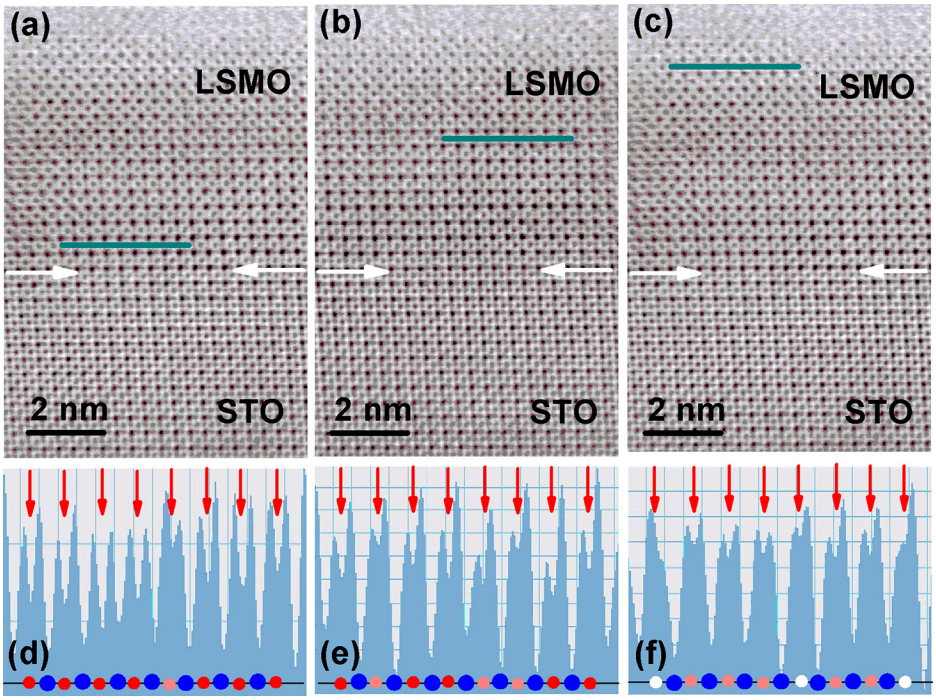

FIG. 2. (a)–(c) The cross-sectional ABF micrographs of the as-grown LSMO film with a thickness of 16 u.c. taken by an aberration-corrected STEM. (d)–(f) The line profiles along the Mn-O-Mn chains (the dark cyan bars) in (a)–(c), respectively. The white arrows indicate where the interface locates. The red arrows point at the O sites. The blue and red circles indicate Mn and O ions, respectively. The lighter red and white circle indicates the presence of oxygen vacancies.

the dead layer is also thicker at the surface, compared to that at the LSMO/STO interface.

In order to reduce the oxygen vacancies in these as-grown films, a treatment of annealing in oxygen atmosphere at 900 °C for 4 h was applied to each sample. The SXRD results show that the *c*-axis lattice constants of the LSMO films can be markedly tuned from larger than that of the STO substrates to smaller by the annealing treatment, which is in accordance with the above conclusion that the unusually large *c*-axis lattice constant is due to the existence of oxygen vacancies in the as-grown films. The smaller value of the *c*-axis than that of the bulk for thinner films after annealing should be caused by the stress from the larger constant in STO substrate. Since it was found in previous works[18,26] that the *c*-axis lattice constant varied with the alteration of the oxygen content in manganite films, the annealing process we performed can greatly compensate the oxygen vacancies in the as-grown films, leading to a contraction of the lattice and variation of strain states in LSMO films. The annealing of manganite films has been reported to affect both the magnetic[15,27–29] and magnetoelectric transport[10,28] properties significantly due to the lattice distortion and reconfiguration of magnetic domains.[30]

Figures 3(a)–3(c) are the cross-sectional ABF micrographs of the annealed LSMO film with the thickness of 16 u.c., while Figures 3(d)–3(f) are the corresponding line profiles along the Mn-O-Mn chains (the dark cyan bars) in Figures 3(a)–3(c), respectively. The same distribution trend of oxygen vacancies along *c* axis as that in the as-grown LSMO film shown in Figure 2 was also found in the annealed film shown in Figure 3, whereas many of the oxygen vacancies inside the LSMO films and around the surfaces have been complemented, as revealed from comparison of the ABF images of the as-grown film shown in Figure 2 and the annealed film shown in Figure 3. The distribution of oxygen vacancies along *c* axis in both the as-grown and annealed films is of vital importance for the physical nature and suggests the application potential of LSMO ultrathin films.[31]

Figures 1(d) and 1(e) display the hysteresis loops (10 K) and temperature-dependent magnetization (20 Oe, field cooling) of the annealed films. Compared with the results of the as-grown films in Figures 1(a) and 1(b), the much larger T_C and M_S of the annealed LSMO films suggest that the annealing process can effectively increase the oxygen content and enhance the double-exchange interactions between Mn^{3+} and M^{4+} in the LSMO films, while the smaller coercivity suggests that the contraction of the lattice induced by the annealing process can change the strain state and facilitate the rotation of the magnetization in LSMO films. It is noticeable that the higher T_C of the annealed films than that of the bulk is a very important advantage for spintronics applications. In our experiment, higher annealing temperature can facilitate the complement of oxygen vacancies and improve the magnetic properties of LSMO film, but no significant improvement was found when it exceeded 900 °C.

The T_C and M_S of these annealed films deduced from Figures 1(d) and 1(e) were plotted in Figure 1(f). It can been seen that both T_C and M_S become larger with the thicknesses of the annealed LSMO films decreasing from 200 to 50 u.c. but vary conversely with further decrease of the thicknesses for annealed LSMO films. We think there are two main factors that influence the variation of the T_C and M_S. One is the interface effect that becomes more pronounced as the films become thinner, the other is the effect of complementing oxygen vacancies through the annealing treatment that becomes more difficult as the films become thicker. Therefore, the interface effect lowers the T_C and M_S with the decreasing film thickness, while the complement of oxygen vacancies leads to the opposite trend. The critical thickness of about 50 u.c. in Figure 1(f), with different variation trends of the T_C and M_S below and above it, indicates that the

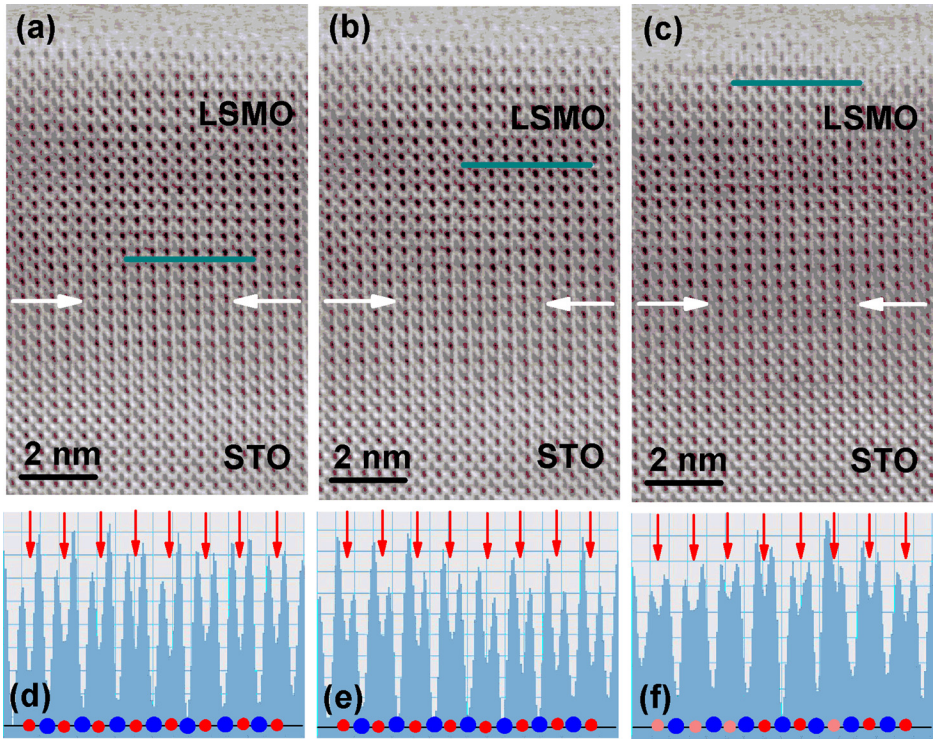

FIG. 3. (a)–(c) The cross-sectional ABF micrographs of the annealed LSMO film with a thickness of 16 u.c. taken by an aberration-corrected STEM. (d)–(f) The line profiles along the Mn-O-Mn chains (the dark cyan bars) in (a)–(c), respectively. The white arrows indicate where the interface locates. The red arrows point at the O sites. The blue and red circles indicate Mn and O ions, respectively. The lighter red and white circle indicates the presence of oxygen vacancies.

influence from the interface seems to dominate in the annealed films with their thicknesses below 20 u.c., whereas the effects of complementing oxygen vacancies through annealing treatment dominate in the annealed films with their thicknesses above 50 u.c. The highest Curie temperature (up to 325 K), much higher than that of 140 K reported for LSMO bulk,[12] was obtained in the annealed LSMO films with the thickness of 50 u.c. as shown in Figure 1(f). Such high T_C in LSMO films means a ferromagnetic device can work at room temperature. A maximum of M_S was also obtained in the LSMO films with the thickness of 50 u.c. as shown in Figure 1(f). Moreover, the ferromagnetic-paramagnetic phase transition still exists in the annealed LSMO films with the thicknesses lower than the reported critical thicknesses of the dead layers in previous works[15,27] with the values from several to tens of nanometers; whereas no detectable sign of ferromagnetism was observed in the ultrathin films with the thickness of 6 u.c. in our experiments. Several series of manganite films were grown and annealed, and the variation trends of the T_C and M_S were measured to be repeatable.

In conclusion, we systematically studied the structural and magnetic properties of LSMO ultrathin films with their thicknesses varying from 200 to 6 u.c. and found that the oxygen vacancies around the surfaces were much more than that close to the interfaces. Many of the oxygen vacancies inside the LSMO films and around the surfaces are complemented by annealing the as-grown samples in oxygen atmosphere. It was also found that the annealing treatment could induce a contraction of the lattice and variation of the strain states in LSMO films and significantly enhance T_C and M_S by complementing the oxygen vacancies in LSMO ultrathin films. The highest Curie temperature and the maximum of the saturation magnetization were obtained in the annealed LSMO films with the thickness of 50 u.c. (about 20 nm). Such a high T_C of LSMO films (up to 325 K), much higher than that of 140 K reported for the LSMO bulk, means a ferromagnetic device can work at room temperature. Our results strongly demonstrate that the interface effect and oxygen content play crucial roles for the intriguing properties of the ultrathin LSMO films, which could be further exploited for advanced functional devices based on ultrathin films of perovskite-type oxides.

This work was supported by the National Basic Research Program of China (No. 2012CB921403) and the National Natural Science Foundation of China (Nos. 10825418, 11134012, and 11004238). The XRD measurement was supported by the Shanghai Synchrotron Radiation Facility (SSRF).

[1]M. Bibes, J. E. Villegas, and A. Barthelemy, Adv. Phys. **60**, 5 (2011).
[2]J. Mannhart and D. G. Schlom, Science **327**, 1607 (2010).
[3]K. J. Jin, H. B. Lu, K. Zhao, C. Ge, M. He, and G. Z. Yang, Adv. Mater. **21**, 4636 (2009).
[4]A. Ohtomo and H. Y. Hwang, Nature **427**, 423 (2004).
[5]T. Koida, M. Lippmaa, T. Fukumura, K. Itaka, Y. Matsumoto, M. Kawasaki, and H. Koinuma, Phys. Rev. B **66**, 144418 (2002).
[6]I. Zutic, J. Fabian, and S. D. Sarma, Rev. Mod. Phys.**76**, 323 (2004).
[7]M. Bibes and A. Barthelemy, IEEE Trans. Electron Devices **54**, 1003 (2007).
[8]S. Valencia, Z. Konstantinovic, D. Schmitz, A. Gaupp, LI. Balcells, and B. Martínez, Phys. Rev. B **84**, 024413 (2011).
[9]A. P. Ramirez, J. Phys.: Condens. Matter **9**, 8171 (1997).
[10]J. M. D. Coey, M. Viret, and S. V. Molnar, Adv. Phys. **48**, 167 (1999).
[11]M. B. Salamon and M. Jaime, Rev. Mod. Phys. **73**, 583 (2001).
[12]A. M. H. Gosnet and J. P. Renard, J. Phys. D: Appl. Phys. **36**, 127 (2003).
[13]A. Biswas, M. Rajeswari, R. C. Srivastava, Y. H. Li, T. Venkatesan, and R. L. Greene, Phys. Rev. B **61**, 9665 (2000).
[14]J. H. Park, E. Vescovo, H. J. Kim, C. Kwon, R. Ramesh, and T. Venkatesan, Phys. Rev. Lett. **81**, 1953 (1998).
[15]J. Z. Sun, D. W. Abraham, R. A. Rao, and C. B. Eom, Appl. Phys. Lett. **74**, 3017 (1999).

[16]C. Wang, K. J. Jin, R. Q. Zhao, H. B. Lu, H. Z. Guo, C. Ge, M. He, C. Wang, and G. Z. Yang, Appl. Phys. Lett. **98**, 181101 (2011).
[17]Y. Tokura, Y. Tomioka, H. Kuwahara, A. Asamitsu, Y. Moritomo, and M. Kasai, J. Appl. Phys. **79**, 5288 (1996).
[18]Z. T. Xu, K. J. Jin, L. Gu, Y. L. Jin, C. Ge, C. Wang, H. Z. Guo, H. B. Lu, R. Q. Zhao, and G. Z. Yang, Small **8**, 1279 (2012).
[19]H. W. Zandbergen, S. Freisem, T. Nojima, and J. Aarts, Phys. Rev. B **60**, 10259 (1999).
[20]M. Izumi, Y. Konishi, T. Nishihara, S. Hayashi, M. Shinohara, and Y. Tokura, Appl. Phys. Lett. **73**, 2497 (1998).
[21]R. Shiozaki, K. Takenaka, Y. Sawaki, and S. Sugai, Phys. Rev. B **63**, 184419 (2001).
[22]T. L. Aselage, D. Emin, S. S. McCready, E. L. Venturini, M. A. Rodriguez, J. A. Voigt, and T. J. Headley, Phys. Rev. B **68**, 134448 (2003).
[23]S. Picozzi, C. Ma, Z. Yang, R. Bertacco, M. Cantoni, A. Cattoni, D. Petti, S. Brivio, and F. Ciccacci, Phys. Rev. B **75**, 094418 (2007).
[24]C. L. Jia and K. Urban, Science **303**, 2001 (2004).
[25]O. L. Krivanek, F. C. Matthew, N. Valeria, J. P. Timothy, J. C. George, D. Niklas, S. O. Christopher, S. S. Zoltan, P. O. Mark, T. P. Sokrates, and J. P. Stephen, Nature **464**, 571 (2010).
[26]P. Orgiani, A. Y. Petrov, R. Ciancio, A. Galdi, L. Maritato, and B. A. Davidson, Appl. Phys. Lett. **100**, 042404 (2012).
[27]J. Dho, N. H. Hur, I. S. Kim, and Y. K. Park, J. Appl. Phys. **94**, 7670 (2003).
[28]H. L. Ju, C. Kwon, Q. Li, R. L. Greene, and T. Venkatesan, Appl. Phys. Lett. **65**, 2108 (1994).
[29]Y. S. Du, B. Wang, T. Li, D. B. Yu, and H. Yan, J. Magn. Magn. Mater. **297**, 88 (2006).
[30]S. R. Bakaul, W. Lin, and T. Wu, Appl. Phys. Lett. **100**, 012403 (2012).
[31]M. Huijben, L. W. Martin, Y. H. Chu, M. B. Holcomb, P. Yu, G. Rijnders, D. H. A. Blank, and R. Ramesh, Phys. Rev. B **78**, 094413 (2008).